

# Effect of Strontium concentration on the luminescent properties of $(\text{Ba}_{1-x}\text{Sr}_x)_2\text{SiO}_4:\text{Eu}^{2+}$ prepared by pressure-assisted combustion-synthesis

Manuel R. Romero-Sandoval<sup>1,†</sup>, M.T. Martínez-Martínez<sup>2,†</sup>, C.R. García<sup>3</sup>, G.A. Hirata-Flores<sup>4\*</sup>

<sup>1,2,4</sup>Centro de Nanociencias y Nanotecnología, Universidad Nacional Autónoma de México, Carretera Tijuana-Ensenada Km. 107, Pedregal Playitas, 22860, Ensenada B.C., México.

<sup>3</sup>Facultad de Ciencias Físico-Matemáticas, Universidad Autónoma de Coahuila Unidad Camporredondo, Coahuila, México.

<sup>†</sup> These authors contributed equally to this work.

\* Corresponding author

**Abstract**— In this work, the effect of Sr doping concentration on the morphological and luminescence properties of  $\text{Ba}_2\text{SiO}_4:\text{Eu}^{2+}$  phosphors was studied. Green-yellow emitting phosphors  $(\text{Ba}_{1-x}\text{Sr}_x)_2\text{SiO}_4$  activated with  $\text{Eu}^{2+}$  ions were fabricated by pressure-assisted combustion synthesis (PACS) at an initial pressure of 3.4 MPa. The Sr (x) atomic concentration was changed from 0.0 to 0.5 at.%. The X-ray diffraction (XRD) analysis showed that these phosphors have a single phase corresponding to the  $\text{Ba}_2\text{SiO}_4$  orthorhombic phase. Different morphologies with sizes in the range of 1-12.12  $\mu\text{m}$  were observed according to the Sr content, such as spheres-like (x=0.0 at.%), irregular-shaped (x=0.2 at.%) and rectangular flakes-like particles (x=0.5 at.%). The main emission bands were located in the range of 507 to 522 nm, which correspond to 4f-5d allowed electric-dipole transition of  $\text{Eu}^{2+}$  and the main excitation band was located at 397 nm. The phosphor with flakes-like morphology (x=0.5 at.% of Sr) exhibited the highest luminescent intensity and its CIE coordinates are (0.31, 0.60) which color is located in the green region. The strong green-yellow emission observed in our phosphors suggests that they can be useful for the green component in RGB white LEDs.

**Keywords**—  $(\text{BaSr})_2\text{SiO}_4$ , combustion synthesis, luminescence, phosphors, white light-emitting diodes (WLEDs).

## I. INTRODUCTION

It is well known that  $(\text{BaSr})_2\text{SiO}_4:\text{Eu}^{2+}$  phosphors powders emit a green-yellow color, therefore, they have a great potential to be used as the green component in white light-emitting diodes (WLEDs) [1]. One approach currently used to fabricate WLEDs is based on the mixture of the blue light produced by a blue LED and the green-yellow light of  $\text{YAG}:\text{Ce}^{3+}$  phosphors [2]. However, this approach presents two disadvantages: 1) this white emission has low color rendering index (CRI  $\uparrow$ 75) [3] and 2) the lacking of red color component, because the most used  $\text{YAG}:\text{Ce}^{3+}$  phosphor for the commercial WLEDs, have a poor red emission [4]. To solve this, a new WLED design has been proposed which includes the blue, red and green components when are excited with near-UV light [5]. Recent reports show that this approach is promising to get good color rendering index ( $\uparrow$ 90) which is suitable for many lighting applications [5-6]. Thus, new blue, green and red phosphors excited with near-UV light are required for this new configuration [7-9]. Most of common phosphors used in lighting present phosphorescence (i.e.  $\text{SrAl}_2\text{O}_4:\text{Eu}^{2+}$ ) which is not desirable for WLEDs and fluorescent lamps applications, thus, the search of green fluorescent emitting phosphor is still a challenge for materials science [10]. In order to solve this problem, the  $\text{Ba}_2\text{SiO}_4:\text{Eu}^{2+}$  green phosphor has been considered as a potential candidate for the green component in WLEDs. The  $\text{Ba}_2\text{SiO}_4:\text{Eu}^{2+}$  material has been synthesized by solid state method [11], co-precipitation, and combustion synthesis [12]. On the one hand, the fabrication of phosphors obtained via solid-state reactions involves very high temperatures with subsequent grinding and milling procedures. Particles prepared by such techniques exhibit many surface defects and large particle size distributions, which can inhibit their luminescent efficiency [13].

Several synthesis procedures have been published to obtain efficient phosphors that can be combined with the blue component from a chip to produce WLEDs. Recently the pressure-assisted combustion synthesis (PACS) [14] has been used to produce luminescent materials with strong brightness. The PACS method is simple, low cost and the materials obtained by this method exhibit high purity and crystallinity [15, 16]. In addition, the PACS synthesis has been used to introduce dopants easier in comparison with normal combustion synthesis because the pressure induces a fast transformation in the combustion process [16]. Thus, this work reports the synthesis of  $(\text{Ba}_{1-x}\text{Sr}_x)_2\text{SiO}_4:\text{Eu}^{2+}$  phosphors fabricated by a pressure-assisted combustion reaction technique (PACS) which has not been explored to produce the  $(\text{Ba}_{1-x}\text{Sr}_x)_2\text{SiO}_4:\text{Eu}^{2+}$  material to the best

of knowledge. Furthermore, we study the influence of the Strontium concentration on the morphology and the luminescent properties of  $(\text{Ba}_{1-x}\text{Sr}_x)_2\text{SiO}_4:\text{Eu}^{2+}$  phosphors excited under near-UV light.

## II. MATERIALS AND METHODS

Europium activated orthosilicates  $(\text{Ba}_{1-x}\text{Sr}_x)_2\text{SiO}_4:\text{Eu}^{2+}$  phosphors powders were prepared by pressure-assisted combustion-synthesis (PACS) reaction. The precursors were adjusted to an appropriate stoichiometric ratio [17]. Europium nitrate  $[\text{Eu}(\text{NO}_3)_3 \cdot 6\text{H}_2\text{O}$  Reaction 99.99%], Barium nitrate  $[\text{Ba}(\text{NO}_3)_2 \cdot \text{Puratronic}$  99.99%], Strontium nitrate  $[\text{Sr}(\text{NO}_3)_3 \cdot \text{Puratronic}$  99.99%] and Silica  $\text{SiO}_2$ , were dissolved in a beaker with deionized water (25 mL) and to obtain a homogeneous mixture we used a magnetic stirrer for 15 minutes. Next, hydrazine  $\text{N}_2\text{H}_4$  was added to obtain a solution. The addition of hydrazine ( $\text{N}_2\text{H}_4$ - reducing agent) has a double purpose: it helps to prevent contamination [18] and also is added as a free carbon fuel. A value of 0.03 atomic concentration (at.) of Eu was fixed while the x atomic concentration of Sr was varied from  $x= 0.0, 0.2$  and 0.5 at.% in order to study the effect of Sr on the luminescent and morphological properties.

### 2.1 PACS Method

Once the precursor solution was obtained, it was placed in a closed batch reactor, the pressure in the reactor was maintained at 3.4 MPa approximately during the reaction time, and then we followed the procedure described in the experimental section of previous reports where the PACS technique is used [14, 15, 16]. After this procedure, we obtained white powders doped with  $\text{Eu}^{3+}$ .

### 2.2 Thermal Annealing

In order to reduce  $\text{Eu}^{3+}$  to  $\text{Eu}^{2+}$ , a thermal annealing of the obtained powders was performed under a reducing atmosphere. The use of reducing atmospheres of  $\text{H}_2$ ,  $\text{N}_2/\text{H}_2$ ,  $\text{NH}_3$  and their combinations are widely used [19, 20]. The thermal annealing of the synthesized powders was performed in a tubular furnace at 1200 °C for 2 h, using  $\text{N}_2/\text{H}_2$  as a reducing gas, with a constant flow of 40 sccm. After the thermal treatment, we obtained green-yellow phosphors powders of  $(\text{Ba}_{1-x}\text{Sr}_x)_2\text{SiO}_4:\text{Eu}^{2+}$  with different concentrations of Sr:  $x = 0.0, 0.2$ , and 0.5 at.%.

### 2.3 Characterization

The crystal structures of the particles were analyzed by a powder X-ray diffractometer (Philips X'pert) employing  $\text{CuK}\alpha$  radiation ( $\lambda = 0.15406$  nm). The measurements were taken in a range of  $2\theta = 20-60^\circ$  with a step size of  $0.02^\circ$  and 1 sec dwell per point. The XRD patterns of particles were confirmed by comparing with the Joint Committee on Power Diffraction Standards (JCPDS) data. The morphology of these samples was observed by using a scanning electron microscope (SEM) JEOL JIB-4500 Multi Beam System.

Cathodoluminescence (CL) images and spectra were collected with a Gatan Mono CL4 detector attached to a Jeol JIB-4500 Multi Beam System. Cathodoluminescent emission was obtained by exciting with an electron beam with an energy of 900 V. The dwell time per pixel was 0.5 sec.

Photoluminescence emission (PL) and excitation (PLE) properties were studied with a fluorescence spectrophotometer (Hitachi F-7000), using a Xe lamp of 450 watts as an excitation source. All measurements were carried out at room temperature. The Commission International de l'Eclairage (CIE) chromaticity coordinates for all samples were calculated from the emission spectra, taking the maximum peak for each sample and following the procedure described in [21].

## III. RESULTS AND DISCUSSION

### 3.1 X-Ray diffraction

The XRD patterns of the  $(\text{Ba}_{1-x}\text{Sr}_x)_2\text{SiO}_4:\text{Eu}^{2+}$  phosphors in Fig. 1a and Fig. 1b indicate that our samples have an orthorhombic phase, (JCPDS Card 077-0150). When  $\text{Sr}^{2+}$  (0.2 at.%) is added the diffraction peaks shift toward higher angles ( $\Delta 2\theta = 0.64^\circ$ ) due to the substitution of  $\text{Ba}^{2+}$  ions (1.34 Å) by smaller  $\text{Sr}^{2+}$  ions (1.12 Å) in the crystal lattice (Fig. 1c) [22], since  $\text{Sr}^{2+}$  ions are smaller than the  $\text{Ba}^{2+}$  ions the lattice is under tensile strain and the diffraction peaks are shifted to the right. This also confirms the incorporation of  $\text{Sr}^{2+}$  ions in the  $\text{Ba}_2\text{SiO}_4:\text{Eu}^{2+}$  lattice. Moreover, the crystalline quality of  $\text{Ba}_2\text{SiO}_4:\text{Eu}^{2+}$  doped decreases when the  $\text{Sr}^{2+}$  is added, as can be confirmed observing the broadening of the peaks on Fig. 1c. For the higher  $\text{Sr}^{2+}$  content (0.5 at.%) the XRD peaks also shifts to higher angles with an increase of  $\Delta 2\theta = 0.24^\circ$  as observed

in Fig. 1d. Furthermore, as the concentration of  $\text{Sr}^{2+}$  increases, the intensity of several diffraction peaks increases leading to improvements in the crystallinity of the obtained phosphors.

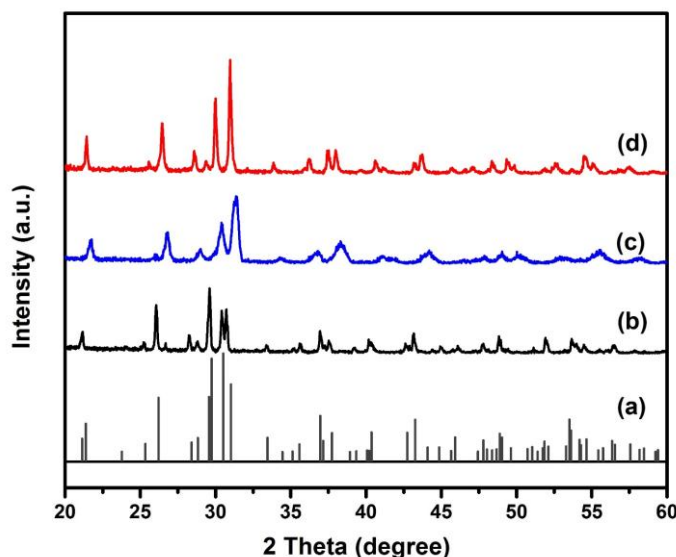


**FIGURE 1. XRD PATTERNS OF THE  $(\text{Ba}_{1-x}\text{Sr}_x)_2\text{SiO}_4:\text{Eu}^{2+}$  PHOSPHORS. (A)  $\text{Ba}_2\text{SiO}_4$ -JCPDS CARD 077-0150, (b)  $\text{Ba}_2\text{SiO}_4:\text{Eu}^{2+}$ , (c)  $(\text{Ba}_{0.8}\text{Sr}_{0.2})_2\text{SiO}_4:\text{Eu}^{2+}$ , (d)  $(\text{Ba}_{0.5}\text{Sr}_{0.5})_2\text{SiO}_4:\text{Eu}^{2+}$ .**

The peaks which corresponds to the crystal planes (200) (102) and (121) of the  $\text{Ba}_2\text{SiO}_4$  phase where selected to calculate the lattice parameters using Bragg's Law. The lattice parameters and the unit cell volume of the samples are shown in Table 1.

**TABLE 1**

**LATTICE PARAMETERS AND CELL VOLUME OF DIFFERENT SAMPLES CALCULATED FROM XRD RESULTS.**

Sample	a (Å)	b (Å)	c (Å)	Cell volume (Å <sup>3</sup> )
$\text{Ba}_2\text{SiO}_4:\text{Eu}^{2+}$	5.8143	10.2113	7.5245	446.7413
$(\text{Ba}_{0.8}\text{Sr}_{0.2})_2\text{SiO}_4:\text{Eu}^{2+}$	5.6986	9.8550	7.3064	410.3252
$(\text{Ba}_{0.5}\text{Sr}_{0.5})_2\text{SiO}_4:\text{Eu}^{2+}$	5.7703	10.0006	7.4168	427.9972

As can be seen from the estimated data, the lattice parameters and unit cell volume values for the doped  $(\text{Ba}_{1-x}\text{Sr}_x)_2\text{SiO}_4:\text{Eu}^{2+}$  phosphors deviate considerably from those of the undoped sample due to the incorporation of  $\text{Sr}^{2+}$  ions into the  $\text{Ba}_2\text{SiO}_4$  lattice, which induces the local distortion of the crystal structure. Fig. 2 shows the plotted values of the calculated orthorhombic lattice parameters as a function of the  $\text{Sr}^{2+}$  content  $x$  in the  $(\text{Ba}_{1-x}\text{Sr}_x)_2\text{SiO}_4:\text{Eu}^{2+}$  phosphors. It is observed that the lattice parameters decrease for the concentration of  $x = 0.2$  at.% Sr and then slightly increase with the concentration of  $x = 0.5$  at.% Sr, this behavior could be explained due to the difference between the electronegativities of Ba and Sr which are: Sr 0.97 and Ba 0.89 (Pauling electronegativity). That means that Sr could trap electrons more efficiently than Ba, and since we are introducing Sr into the  $\text{Ba}_2\text{SiO}_4$  as a consequence the lattice volume increases.

### 3.2 Morphology of $(\text{Ba}_{1-x}\text{Sr}_x)_2\text{SiO}_4:\text{Eu}^{2+}$ phosphors and CL images

The morphology of the  $\text{Ba}_2\text{SiO}_4:\text{Eu}^{2+}$  phosphors doped with different Sr concentrations is shown in Fig. 3. The sample without Sr in Fig. 3a exhibited a mixture of irregular-shaped particles and some spheres-like particles. The histogram of Fig. 3b shows the particle size distribution of the  $\text{Ba}_2\text{SiO}_4:\text{Eu}^{2+}$  phosphors fitted by one Gaussian curve. From the size distribution histogram, an average size of  $7.58 \pm 3 \mu\text{m}$  was estimated. The morphology of phosphors with a concentration of 0.2 at.% of Sr ( $(\text{Ba}_{0.8}\text{Sr}_{0.2})_2\text{SiO}_4:\text{Eu}^{2+}$ ) is depicted in Fig. 3c, it consists of irregular-shaped particles. The average size of the  $(\text{Ba}_{0.8}\text{Sr}_{0.2})_2\text{SiO}_4:\text{Eu}^{2+}$  phosphors was calculated using a histogram fitted by two Gaussian curves (Fig. 3d). The two average sizes estimated were  $18.4 \pm 3.7 \mu\text{m}$  and  $8.3 \pm 2.8 \mu\text{m}$ . Fig. 3e shows the morphology of the  $(\text{Ba}_{0.5}\text{Sr}_{0.5})_2\text{SiO}_4:\text{Eu}^{2+}$  phosphors, consisting mainly of flakes-like powders. The average sizes of the  $(\text{Ba}_{0.5}\text{Sr}_{0.5})_2\text{SiO}_4:\text{Eu}^{2+}$  phosphors were estimated with the

histogram and corresponding Gaussian fits of the data in Fig. 3f, the average width calculated was  $8.84 \pm 3.2 \mu\text{m}$  and the average length was  $12.12 \pm 4 \mu\text{m}$ .

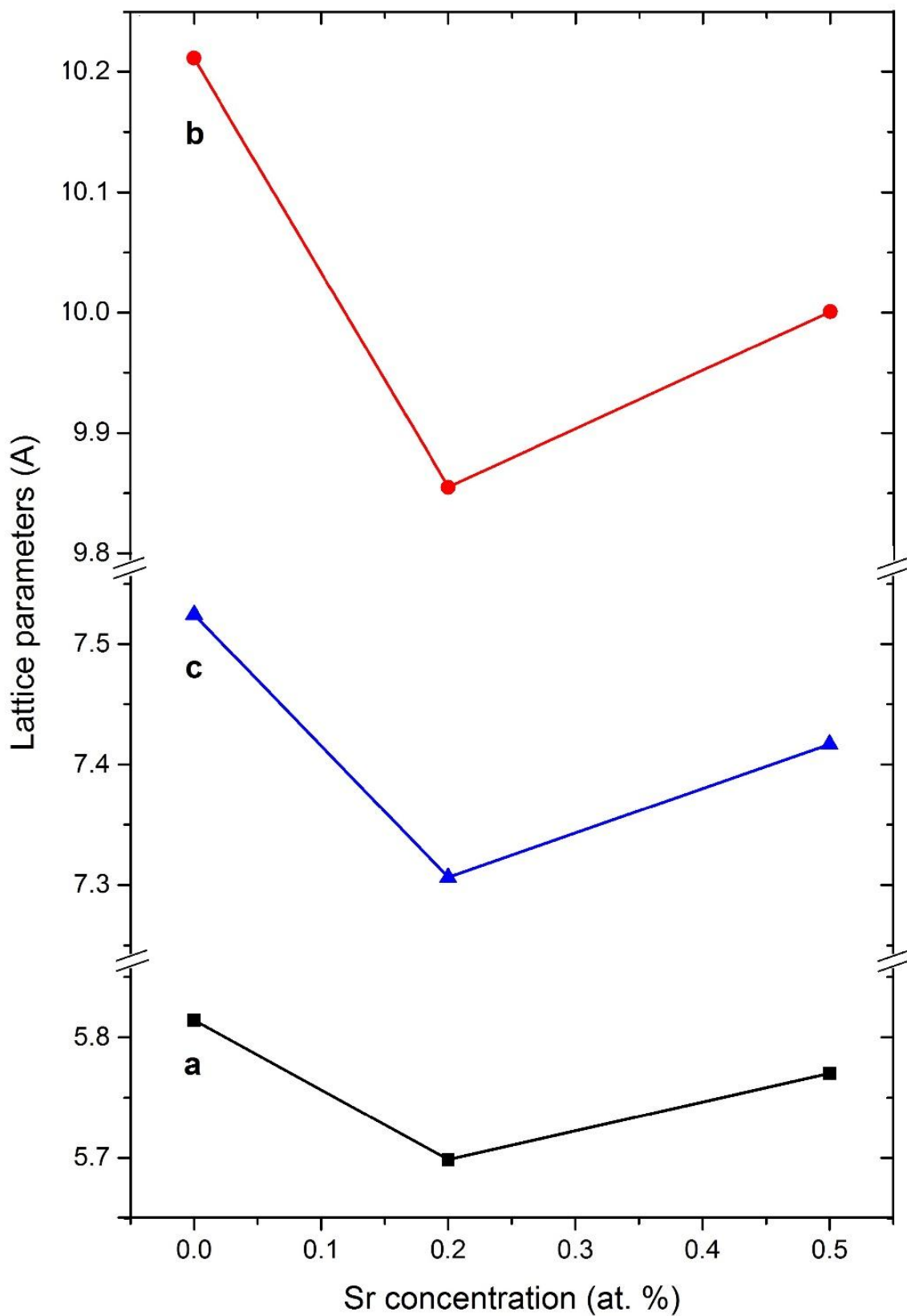
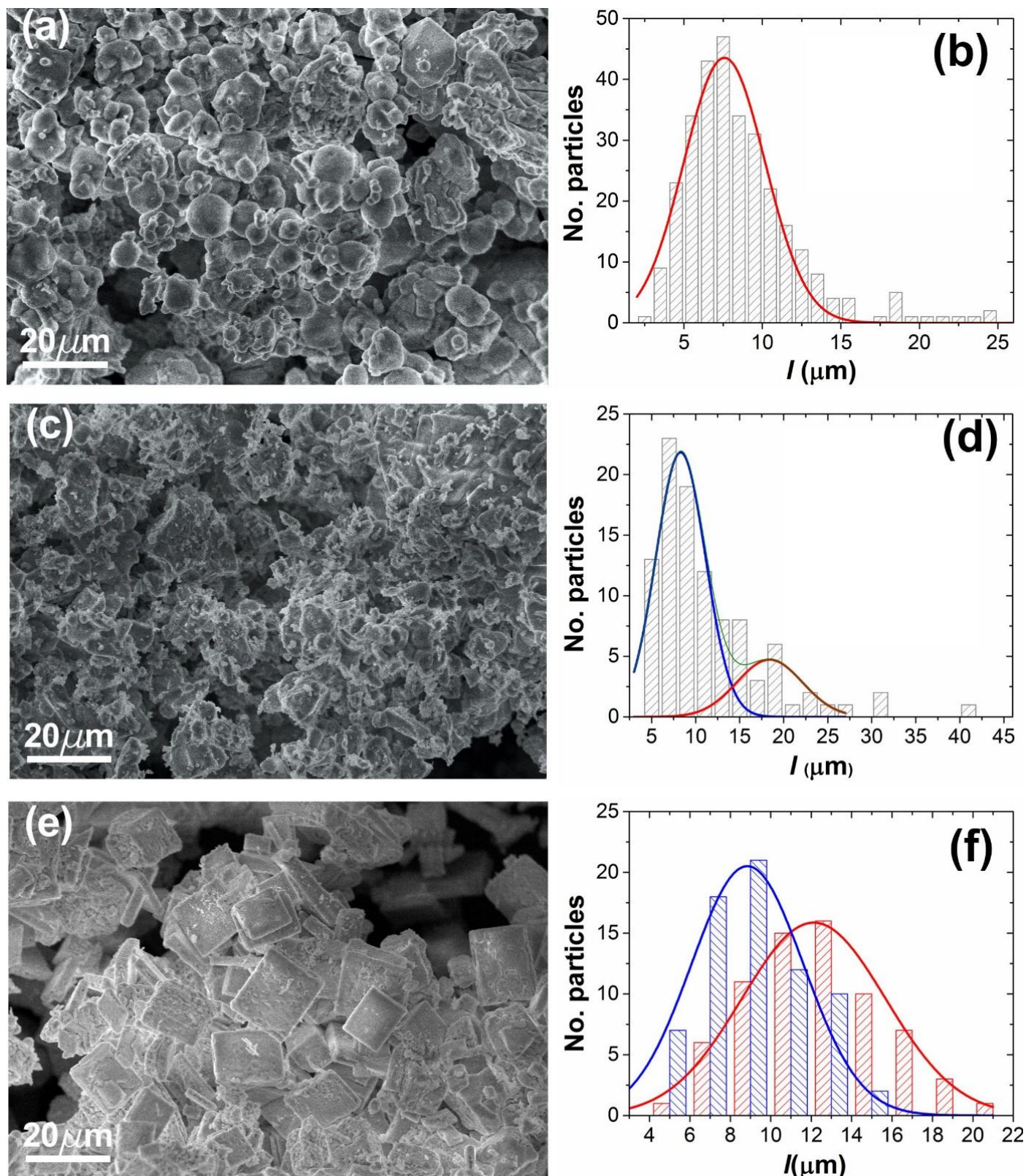


FIGURE 2. PLOT OF THE LATTICE PARAMETERS A, B AND C AS A FUNCTION OF  $\text{Sr}^{2+}$  CONTENT X IN THE  $(\text{Ba}_{1-x}\text{Sr}_x)_2\text{SiO}_4:\text{Eu}^{2+}$  PHOSPHORS.



**FIGURE 3. SEM IMAGES AND PARTICLE SIZE DISTRIBUTION HISTOGRAMS OF THE  $(\text{Ba}_{1-x}\text{Sr}_x)_2\text{SiO}_4:\text{Eu}^{2+}$  PHOSPHORS OBTAINED BY PACS WITH DIFFERENT CONCENTRATIONS OF SR: (A)  $\text{Ba}_2\text{SiO}_4:\text{Eu}^{2+}$ , (B)  $(\text{Ba}_{0.8}\text{Sr}_{0.2})_2\text{SiO}_4:\text{Eu}^{2+}$  AND (C)  $(\text{Ba}_{0.5}\text{Sr}_{0.5})_2\text{SiO}_4:\text{Eu}^{2+}$ ; (D), (E) AND (F) ARE THEIR CORRESPONDING SIZE DISTRIBUTION HISTOGRAMS.**

As observed in the SEM micrographs, an increase of Sr concentration modify the phosphors morphology. For the phosphors without Sr ( $\text{Ba}_2\text{SiO}_4:\text{Eu}^{2+}$ ) the morphology consists mainly of spheres-like powders, for the middle concentration of Sr ( $(\text{Ba}_{0.8}\text{Sr}_{0.2})_2\text{SiO}_4:\text{Eu}^{2+}$ ) the morphology exhibited is composed of agglomerated clusters without a specific shape and finally for the highest concentration of Sr ( $(\text{Ba}_{0.5}\text{Sr}_{0.5})_2\text{SiO}_4:\text{Eu}^{2+}$ ) the morphology presented is flakes-like particles. These results suggest that the particle morphology can be controlled by increasing the Sr concentration, in fact, a change in the morphology of the phosphors induces an enhancement in the cathodoluminescence of Sr-doped  $\text{Ba}_2\text{SiO}_4:\text{Eu}^{2+}$  phosphors as explained in the next section.

### 3.3 CL and PL Spectra

The surface morphology of phosphors is well known to have an effect on the PL response [23]. Cathodoluminescence (CL) can be defined as the emission of light as the result of electron bombardment [24]. An advantage of cathodoluminescence (CL) compared to photoluminescence (PL) is the high spatial resolution that can be achieved.

The brightness of the CL images indicates the distribution of the luminescence centers in the particles. The CL images of the obtained phosphors are shown in Figure 4. For the  $\text{Ba}_2\text{SiO}_4:\text{Eu}^{2+}$  and  $(\text{Ba}_{0.8}\text{Sr}_{0.2})_2\text{SiO}_4:\text{Eu}^{2+}$  phosphors, the CL images demonstrated that the luminescence centers are randomly distributed through the particles, showing some dark spots on the surface of the particles due to low luminescent response at these zones. In the case of the sample  $(\text{Ba}_{0.5}\text{Sr}_{0.5})_2\text{SiO}_4:\text{Eu}^{2+}$ , the luminescence centers are almost all over the particles, comparing it with the phosphors with low Sr concentrations, these present a uniform distribution of the centers of luminescence through all the particle surfaces, consequently the image shows more brightness.

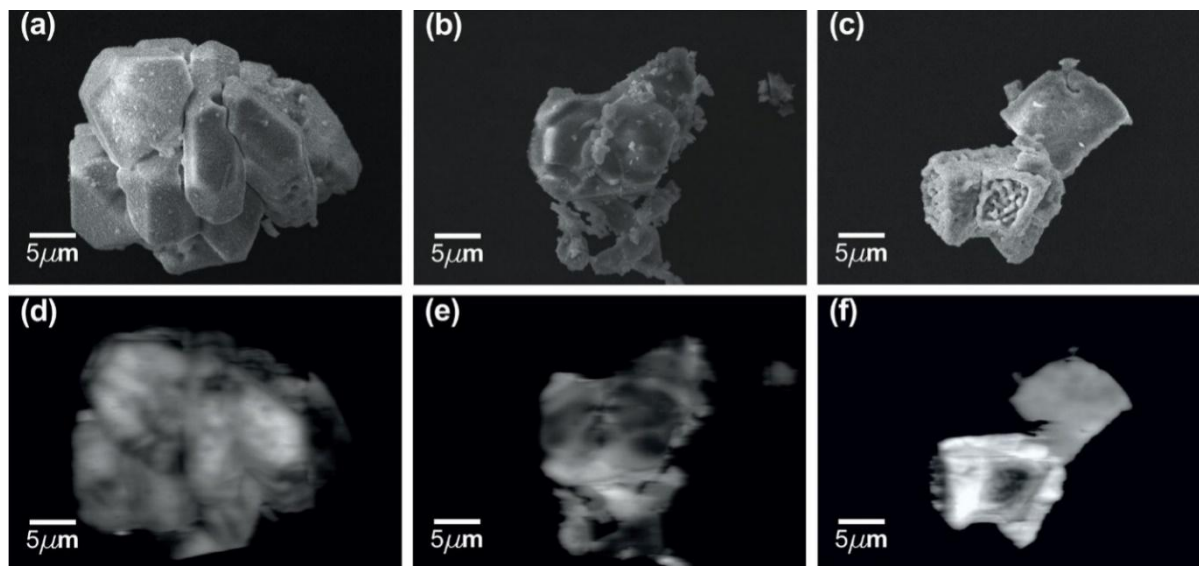
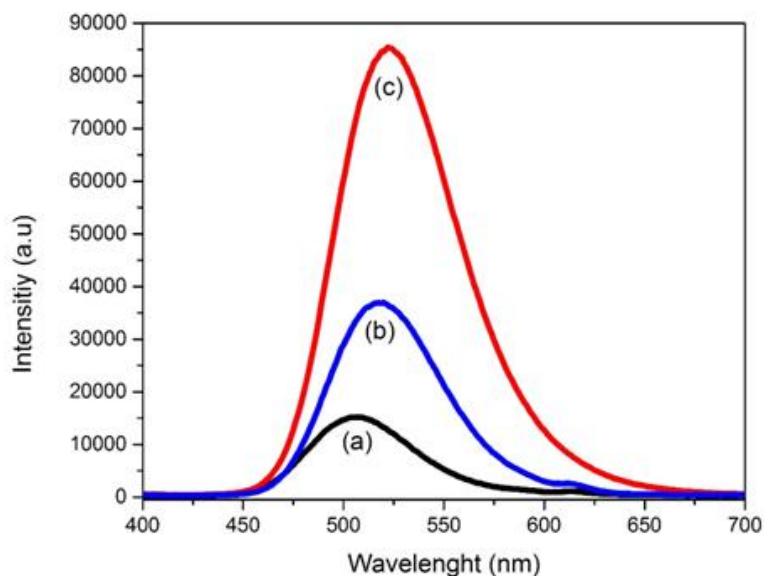


**FIGURE 4. MONOCHROMATIC CL IMAGES OF A SINGLE AGGLOMERATE OF THE  $(\text{Ba}_{1-x}\text{Sr}_x)_2\text{SiO}_4:\text{Eu}^{2+}$  PHOSPHORS WITH DIFFERENT CONCENTRATIONS OF SR: (A) SECONDARY-ELECTRON IMAGE OF  $\text{Ba}_2\text{SiO}_4:\text{Eu}^{2+}$ , (B) SE IMAGE OF  $(\text{Ba}_{0.8}\text{Sr}_{0.2})_2\text{SiO}_4:\text{Eu}^{2+}$ , (C) SE IMAGE OF  $(\text{Ba}_{0.5}\text{Sr}_{0.5})_2\text{SiO}_4:\text{Eu}^{2+}$ , (D), (E), (F) CL IMAGES OF THE RESPECTIVE SE IMAGES.**

In order to evaluate the effect of host composition on the luminescence of the phosphors, we have investigated the CL and PL spectra for a series of  $(\text{Ba}_{1-x}\text{Sr}_x)_2\text{SiO}_4:\text{Eu}^{2+}$  as a function of  $x$  ( $x = 0.0, 0.2$  and  $0.5$  at.%).

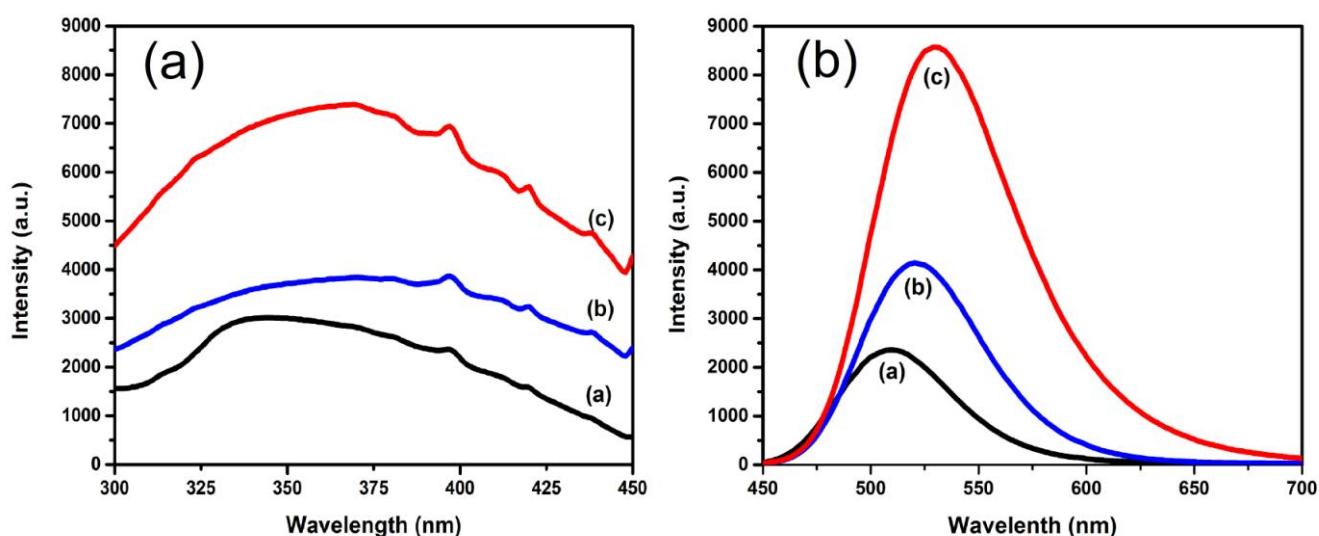
A constant value of 0.03 at.% of  $\text{Eu}^{2+}$  dopant was used in this series of experiments because previous reports demonstrated that an increase in the concentration above 0.03 at.% does not improve the photoluminescence performance[25]. This behavior is due to the concentration quenching, such phenomenon is explained according to the percolation model [26] and can be applicable to the concentration quenching of the compound based on the following assumptions: (1) The interaction between the  $\text{Eu}^{2+}$  ions occurs only among the nearest-neighbor sites in the rare earth sub-lattice; or (2) the concentration quenching is due to the energy transfer from a percolating cluster of  $\text{Eu}^{2+}$  ions to trap centers. For oxide phosphors (as the ones produced in this work) the energy transfers occurs within the nearest  $\text{Eu}^{2+}$  ions [27].

Fig. 5 shows the CL emission spectra of the  $\text{Ba}_2\text{SiO}_4:\text{Eu}^{2+}$  phosphors with different Sr concentrations. The CL spectra demonstrate that an increase in the Sr concentration increases the cathodoluminescence intensity. The  $\text{Ba}_2\text{SiO}_4:\text{Eu}^{2+}$  sample produced the lowest CL intensity. The intensity increases as the Sr concentration increases. Furthermore, as the Sr content increases the emission peak shifts to a larger wavelength, from  $\lambda = 507$  nm for  $\text{Ba}_2\text{SiO}_4:\text{Eu}^{2+}$  to  $\lambda = 522$  nm for  $(\text{Ba}_{0.5}\text{Sr}_{0.5})_2\text{SiO}_4:\text{Eu}^{2+}$ . The shift observed in the maximum of the photoluminescence and cathodoluminescence spectra as a function of the Sr increasing is attributed to the sensitivity of the divalent europium ( $\text{Eu}^{2+}$ ) as a function to the Sr doping into the matrix composition. The emission wavelength range that can be obtained by varying the Sr content in this system is between  $\lambda = 505$  nm up to  $\lambda = 575$  nm [16].



**FIGURE 5. CL SPECTRA OF PHOSPHORS POWDERS PRODUCED BY PACS AT DIFFERENT SR CONCENTRATIONS. (A)  $\text{Ba}_2\text{SiO}_4:\text{Eu}^{2+}$ , (B)  $(\text{Ba}_{0.8}\text{Sr}_{0.2})_2\text{SiO}_4:\text{Eu}^{2+}$ , (C)  $(\text{Ba}_{0.5}\text{Sr}_{0.5})_2\text{SiO}_4:\text{Eu}^{2+}$ .**

The excitation (EX) and emission photoluminescence (PL) spectra of  $(\text{Ba}_{1-x}\text{Sr}_x)_2\text{SiO}_4:\text{Eu}^{2+}$  phosphors prepared by PACS with different Sr concentrations are shown in Fig. 5. The excitation spectra (monitored at 511 nm) (Fig. 6a) exhibit a broad band in the wavelength range from  $\lambda=300$  nm to  $\lambda = 450$  nm, which is due to  $4f^7 (8S7/2) - 4f^65d$  transition of  $\text{Eu}^{2+}$  ions. The  $\text{Eu}^{2+}$  ions located in different sites, experience different crystal field effect on the 5d orbit and have different energy levels, this produce wider absorption bands in the near UV region [28].



**FIGURE 6. PL SPECTRA OF PHOSPHORS POWDERS PRODUCED BY PACS: (A) EXCITATION SPECTRA AT FIXED  $\lambda_{em}$  (507 nm, 517 nm and 522 nm) AND (B) EMISSION SPECTRA EXCITED WITH  $\lambda_{exc} = 397$  nm. FOR BOTH IMAGES (a)  $\text{Ba}_2\text{SiO}_4:\text{Eu}^{2+}$ , (b)  $(\text{Ba}_{0.8}\text{Sr}_{0.2})_2\text{SiO}_4:\text{Eu}^{2+}$ , (c)  $(\text{Ba}_{0.5}\text{Sr}_{0.5})_2\text{SiO}_4:\text{Eu}^{2+}$ .**

The emission spectrum (excited by 254 nm) presents bands peaking at  $\lambda = 507$  nm,  $\lambda = 517$  nm and  $\lambda = 522$  nm for each Sr concentration (Fig. 6b). Those bands are attributed to the  $4f^65d-4f^7$  ( $8S_{7/2}$ ) transitions of  $\text{Eu}^{2+}$  [27], such as transition of  $\text{Eu}^{2+}$  is allowed while exchange interaction is responsible for the energy transfer for forbidden transitions [29].

As we know, the fluorescent mechanism of  $\text{Eu}^{2+}$  in  $(\text{Ba}_{1-x}\text{Sr}_x)_2\text{SiO}_4:\text{Eu}^{2+}$  phosphors is the 4f-5d allowed electric-dipole transition, according with Dexter's theory the process of energy transfer should be controlled by electric multipole-multipole interaction [30]. The intensity of the bands changes depending on the Sr concentration, yielding the highest intensity the  $(\text{Ba}_{0.5}\text{Sr}_{0.5})_2\text{SiO}_4:\text{Eu}^{2+}$  sample.

As the value of Sr concentration increases, a red shift from 507 nm ( $x=0$ ) to 522 nm ( $x=0.5$  at. %) is observed, see the PL spectra of  $(\text{Ba}_{1-x}\text{Sr}_x)_2\text{SiO}_4:\text{Eu}^{2+}$  phosphors. This shift can be attributed to the apparent strengthening of the crystal field and smaller lattice dimensions due to the substitution of  $\text{Ba}^{2+}$  ions for smaller  $\text{Sr}^{2+}$  ions [22]. These phosphors show emission bands in the range from green to yellow (500 nm - 580 nm). The broad emission band indicates a strong coupling interaction between the  $\text{Eu}^{2+}$  and the host which can be attributed to the presence of an excited electron in an outer shell of the  $\text{Eu}^{2+}$  ion [31]. The luminescence spectral feature depends on the relative intensity of the two sites (SI and SII) in the lattices. The crystalline field surrounding the Eu (SII) are stronger than that due to Eu (SI). Consequently, the emissions at 480 nm and 560 were attributed to Eu(I) and Eu(II) respectively. Thus, the emission bands are produced by  $\text{Eu}^{2+}$  ions at different lattice sites. The identified phase for the obtained phosphors is  $\text{Ba}_2\text{SiO}_4$ . In the structure of  $\text{Ba}_2\text{SiO}_4$  there are two different  $\text{Eu}^{2+}$  emissions from the two available sites in the lattice, one is ten coordinated Ba (I) and the other is surrounded by nine oxygen ions. The emission band of  $\text{Ba}_2\text{SiO}_4:\text{Eu}^{2+}$  that presents a maximum at  $\lambda_{em}=507$ nm (Fig. 5a), is attributed to the  $\text{Eu}^{2+}$  ions in the site (SII) [32]. The emission bands of the orthosilicates  $(\text{Ba}_{0.8}\text{Sr}_{0.2})_2\text{SiO}_4:\text{Eu}^{2+}$  and  $(\text{Ba}_{0.5}\text{Sr}_{0.5})_2\text{SiO}_4:\text{Eu}^{2+}$  exhibit a maximum at 517 nm and 522 nm respectively, these lattices have only one alkaline earth site, these long-wavelength emission bands must be due to  $\text{Eu}^{2+}$  on the barium (SI) [33].

The effects of varying the (x) Sr concentration on the emission color can be observed on the Commission Internationale de l'Eclairage (CIE) diagram in Fig. 7. It is clearly seen in the CIE diagram that an increase of the Sr content moves the coordinates from blue-green (point "a") to yellow-green (point "c"). Pictures in the inset of figure 7 were obtained with a band gap filter which cuts the back light reflection from the UV lamp.

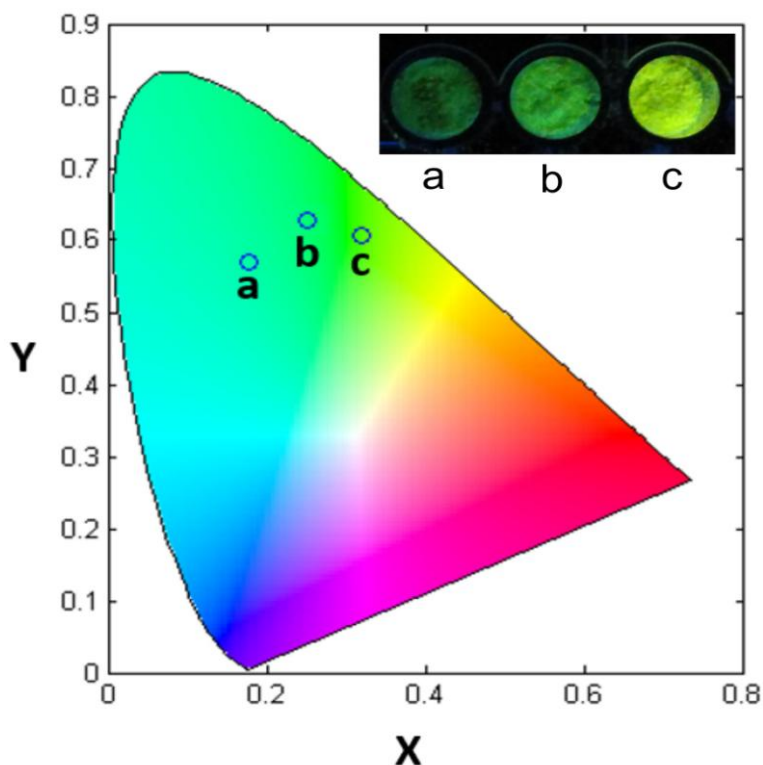


**FIGURE 7. CIE CHROMATICITY DIAGRAM OF THE PHOSPHORS POWDERS  $(\text{Ba}_{1-x}\text{Sr}_x)_2\text{SiO}_4:\text{Eu}^{2+}$  WITH DIFFERENT Sr/Ba RATIO. POINTS (A)  $\text{Ba}_2\text{SiO}_4:\text{Eu}^{2+}$ , (B)  $(\text{Ba}_{0.8}\text{Sr}_{0.2})_2\text{SiO}_4:\text{Eu}^{2+}$ , (C)  $(\text{Ba}_{0.5}\text{Sr}_{0.5})_2\text{SiO}_4:\text{Eu}^{2+}$ . THE INSET SHOWS PHOTOGRAPHS OF THESE PHOSPHORS UNDER 365nm EXCITATION.**

#### IV. CONCLUSIONS

Green-yellow  $(\text{Ba}_{1-x}\text{Sr}_x)_2\text{SiO}_4:\text{Eu}^{2+}$  emitting phosphors were successfully produced by a pressure-assisted combustion synthesis method with strong brightness. The obtained phosphors are single-phase with a  $\text{Ba}_2\text{SiO}_4$  type orthorhombic structure. The phosphors without strontium showed an irregular and agglomerated morphology, whereas that for the higher Sr content the particles presented a flakes-like morphology. According with the CL and PL spectra the phosphors with flakes-like morphology had the highest luminescent intensity, this is because of the smaller specific surface area as compared with granular phosphor. The emission bands ranged from 507 to 522 nm, these emission bands appeared due to the incorporation of the  $\text{Eu}^{2+}$  ions on the barium sites. By introducing Sr atoms into the host lattice the lattice of  $\text{Ba}_2\text{SiO}_4$  is distorted. In consequence, the emission color slightly changed from green to yellow, due to the splitting of the crystal field. Our results indicate that our phosphors are potential candidates for near-UV light excited white LED's.

#### ACKNOWLEDGEMENTS

The authors acknowledged the technical support of E. Aparicio and I. Gradilla.

#### REFERENCES

- [1] J.K. Park, K.J. Choi, K.N. Kim, and C.H. Kim, "Investigation of strontium silicate yellow phosphors for white light emitting diodes from a combinatorial chemistry," *Appl. Phys. Lett.* vol. 87, pp. 031108-031108-3, 2005.
- [2] J.K. Park, M.A. Lim, C.H. Kim, H.D. Park, J.T. Park, and S.Y. Choi, "White light-emitting diodes of GaN-based  $\text{Sr}_2\text{SiO}_4:\text{Eu}$  and the luminescent properties," *Appl. Phys. Lett.* vol. 82, pp. 683-685, 2005.
- [3] X. Li, J.D. Budai, F. Liu, J.Y. Howe, J. Zhang, X.J. Wang, Z. Gu, C. Sun, R.S. Meltzer, and Z. Pan., "New yellow  $\text{Ba}_{0.93}\text{Eu}_{0.07}\text{Al}_2\text{O}_4$  phosphor for warm-white light-emitting diodes through single-emitting-center conversion," *Light: Science & Applications*, vol. 2, pp. e50, 2013.
- [4] L. Wang, X. Zhang, Z. Hao, Y. Luo, X.J. Wang, and J. Zhang, "Enriching red emission of  $\text{Y}_3\text{Al}_5\text{O}_{12}:\text{Ce}^{3+}$  by codoping  $\text{Pr}^{3+}$  and  $\text{Cr}^{3+}$  for improving color rendering of white LEDs," *Opt. Express*, vol. 18, pp. 25177-25182, 2010.
- [5] C.C. Tsai, "Color Rendering Index Thermal Stability Improvement of Glass-Based Phosphor-Converted White Light-Emitting Diodes for Solid-State Lighting," *Int. J. Photoenergy*, pp. 407239-407239, 2014.
- [6] S. Nizamoglu, G. Zengin, and H.V. Demir, "Color-converting combinations of nanocrystal emitters for warm-white light generation with high color rendering index," *Appl. Phys. Lett.*, vol. 92, pp. 031102-031102-3, 2008.
- [7] F.P. Wenzl, C. Sommer, J.R. Krenn, P. Pachler, and P. Hartmann, "White-light engineering of phosphor-converted LEDs," *SPIE*, DOI 10.1117/2.1201010.003158, 2010.
- [8] C. Sun, Y.Y. Chang, T.H. Yang, T.Y. Chung, C.C. Chen, T.X. Lee, D.R. Li, C.Y. Lu, Z.Y. Ting, B. Glorieux, Y.C. Chen, K.Y. Lai, and C.Y. Liu, "Packaging efficiency in phosphor-converted white LEDs and its impact to the limit of luminous efficacy," *J. Sol. State Lighting*, vol. 1, pp. 19, 2014.
- [9] Y. Chen, M. Wang, J. Wang, M. Wu, and C. Wang, "A high color purity red emitting phosphor  $\text{CaYAlO}_4:\text{Mn}^{4+}$  for LEDs," *J. Sol. State Lighting*, vol. 1, pp. 15, 2014.
- [10] Y. Tian, "Development of phosphors with high thermal stability and efficiency for phosphor-converted LEDs," *J. Sol. State Lighting*, vol. 1, pp. 11, 2014.
- [11] M. Zhang, J. Wang, Q. Zhang, W. Ding, and Q. Su, "Optical properties of  $\text{Ba}_2\text{SiO}_4:\text{Eu}^{2+}$  phosphor for green light-emitting diode (LED)," *Materials Research Bulletin*, vol. 42, pp. 33-39, 2007.
- [12] J.K. Han, M.E. Hannah, A. Piquette, G.A. Hirata, J.B. Talbot, K.C. Mishra, and J. McKittrick, "Structure dependent luminescence characterization of green-yellow emitting  $\text{Sr}_2\text{SiO}_4:\text{Eu}^{2+}$  phosphors for near UV LEDs," *J. Luminescence*, vol. 132, pp. 106-109, 2012.
- [13] S. Shionoya, W.M. Yen, and H. Yamamoto, "Phosphor Handbook", CRC Press, 2006, pp. 341-354.
- [14] J.R. Garcia, G.A. Hirata, and J. McKittrick, "New combustion synthesis technique for the production of  $(\text{In}_x\text{Ga}_{1-x})_2\text{O}_3$  powders: Hydrazine/metal nitrate method," *J. Mater. Res.*, vol. 16, pp.1059-1065, 2001.
- [15] C.E. Rodriguez-Garcia, N. Perea-López, G.A. Hirata, and S.P. DenBaars, "Red-emitting  $\text{SrIn}_2\text{O}_4:\text{Eu}^{3+}$  phosphor powders for applications in solid state white lamps," *J. Physics D.*, vol. 41, pp. 092005-4, 2008.
- [16] C.E. Rodríguez-García, N. Perea-López, and G.A. Hirata, "Near UV-Blue Excitable Green-Emitting Nanocrystalline Oxide," *Adv. Mater. Sci. Eng.*, pp. 790517-790517-7, 2011.
- [17] T.L. Barry, "Fluorescence of  $\text{Eu}^{2+}$ -Activated Phases in Binary Alkaline Earth Orthosilicate Systems," *J. Electrochem. Soc.*, vol. 115 pp. 1181-1184, 1968.
- [18] S.R. Jain, K.C. Adiga, and V.R.P. Verneker, "Thermochemistry and lower combustion limit of ammonium perchlorate in presence of methylammonium perchlorates," *Combust. Flame*, vol. 40, pp. 113-120, 1981.
- [19] G.A. Hirata, F.E. Ramos, and J. McKittrick, "Development of luminescent materials with strong UV-blue absorption," *Opt. Mater.* vol. 27, pp. 1301-1304, 2005.
- [20] G.A. Hirata, E.J. Bosze, and J. McKittrick, "Development of nanostructured  $\text{EuAl}_2\text{O}_4$  phosphors with strong long-UV excitation," *J. Nanosci. Nanotechnol.*, vol. 8, pp. 6461-6465, 2008.
- [21] R.J. Mortimer, and T.S. Varley, "Quantification of colour stimuli through the calculation of CIE chromaticity coordinates and luminance data for application to insitu colorimetry studies of electrochromic materials," *Displays*, vol. 32, pp. 35-44, 2011.
- [22] W. Perrin and W.H. Tarn, "Handbook of Metal Etchants," CRC Press Boca Raton, Florida United States of America, 1991, vol. 1, pp.141 and 1199.

- [23] I. Baginskiy, R.S. Lui, C.L. Wang, R.T. Lin, and Y.J. Yao, "Temperature dependent Emission of Strontium-Barium Orthosilicate ( $\text{Sr}_2\text{-Ba}_x\text{SiO}_4\text{:Eu}^{2+}$ ) Phosphors for high-power white light-emitting diodes," *J. Electrochem. Soc.*, vol. 158, pp. 118-121, 2011.
- [24] B.G. Yacobi, and D.B. Holt, "Cathodoluminescence scanning electron microscopy of semiconductors," *J. Appl. Phys.*, vol. 59, pp. R1-R24, 1986.
- [25] C.H. Huang, and T.M. Chen, "Novel Yellow-Emitting  $\text{Sr}_8\text{MgLn}(\text{PO}_4)_7\text{:Eu}^{2+}$  ( $\text{Ln}=\text{Y, La}$ ) Phosphors for Applications in White LEDs with Excellent Color Rendering Index," *Inorg Chem.*, vol. 50, pp. 5725-30, 2011.
- [26] T. Honma, K. Toda, Z.G. Ye, and M. Sato, "Concentration quenching of the  $\text{Eu}^{3+}$ - Activated luminescence in some layered perovskites with two-dimensional arrangement," *J. Phys. Chem. Solids.*, vol. 59, pp. 187-1193, 1998.
- [27] G. Blasse, "Energy transfer in oxidic phosphors," *Physics Letters A.*, vol. 28, pp. 444-445, 1968.
- [28] C.R. Ronda, "Luminescence: From Theory to Applications," WILEY-VCH Verlag GmbH & Co. KGaA, Weinheim, 2008, ISBN: 978-3-527-31402-7, pp. 12-13.
- [29] G. Blasse, and B.C. Grabmaier, "Luminescent Materials," Springer-Verlag, Berlin, 1994, pp. 41.
- [30] V.A. Vyssotsky, S.B. Gordon, H.L. Frisch, and J.M. Hammersley, "Critical Percolation Probabilities (Bond Problem)," *Phys. Rev. Lett.*, vol. 123, pp. 1566, 1961.
- [31] D.L. Dexter, "A Theory of Sensitized Luminescence in Solids," *J. Chem. Phys.*, vol. 21, pp. 836-850, 1953.
- [32] H.D. Nguyena, I.H. Yeob, and S. Mhoa, "Identification of the Two Luminescence Sites of  $\text{Sr}_2\text{SiO}_4\text{:Eu}^{2+}$  and  $(\text{SrBa})_2\text{SiO}_4\text{:Eu}^{2+}$  Phosphors," *ECS Trans.*, vol. 28, pp. 167-173, 2010.
- [33] S.H.M. Poort, W. Janssen, and G. Blasse, "Optical properties of  $\text{Eu}^{2+}$  -activated orthosilicates and orthophosphates," *J. Alloys Compd.*, vol. 260, pp. 93-97, 1997.